

This article was downloaded by:

On: 23 January 2011

Access details: *Access Details: Free Access*

Publisher *Taylor & Francis*

Informa Ltd Registered in England and Wales Registered Number: 1072954 Registered office: Mortimer House, 37-41 Mortimer Street, London W1T 3JH, UK



Journal of Coordination Chemistry

Publication details, including instructions for authors and subscription information:

<http://www.informaworld.com/smpp/title~content=t713455674>

Synthesis, characterization, and formation constant of hexacoordinate iron(III) complexes

Mozaffar Asadi^a; Bahram Hemmateenejad^a; Maryam Mohammadikish^a

^a Department of Chemistry, College of Sciences, Shiraz University, Shiraz 71454, I. R. Iran

First published on: 08 October 2009

To cite this Article Asadi, Mozaffar , Hemmateenejad, Bahram and Mohammadikish, Maryam(2010) 'Synthesis, characterization, and formation constant of hexacoordinate iron(III) complexes', *Journal of Coordination Chemistry*, 63: 1, 124 – 135, First published on: 08 October 2009 (iFirst)

To link to this Article: DOI: 10.1080/00958970903302681

URL: <http://dx.doi.org/10.1080/00958970903302681>

PLEASE SCROLL DOWN FOR ARTICLE

Full terms and conditions of use: <http://www.informaworld.com/terms-and-conditions-of-access.pdf>

This article may be used for research, teaching and private study purposes. Any substantial or systematic reproduction, re-distribution, re-selling, loan or sub-licensing, systematic supply or distribution in any form to anyone is expressly forbidden.

The publisher does not give any warranty express or implied or make any representation that the contents will be complete or accurate or up to date. The accuracy of any instructions, formulae and drug doses should be independently verified with primary sources. The publisher shall not be liable for any loss, actions, claims, proceedings, demand or costs or damages whatsoever or howsoever caused arising directly or indirectly in connection with or arising out of the use of this material.

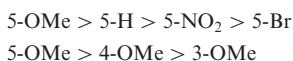
Synthesis, characterization, and formation constant of hexacoordinate iron(III) complexes

MOZAFFAR ASADI*, BAHRAM HEMMATEENEJAD and MARYAM MOHAMMADIKISH

Department of Chemistry, College of Sciences,
Shiraz University, Shiraz 71454, I. R. Iran

(Received 19 January 2009; in final form 10 July 2009)

Twelve iron(III) complexes $[\text{Fe}^{\text{III}}(\text{L}^{\text{X}})_2]\text{ClO}_4$, where $(\text{L}^{\text{X}})^-$ is the deprotonated form of a series of asymmetric ligands containing pyridine and substituted phenol moieties $(\text{XPh}(\text{OH})-\text{CH}=\text{N}-(\text{CH}_2)_n-\text{Py})$ that $\text{X} = \text{H}, 5\text{-Br}, 5\text{-NO}_2, 5\text{-OMe}, 4\text{-OMe}, 3\text{-OMe}$, and $n = 1, 2$, were synthesized and characterized by ^1H NMR, IR, UV-Vis spectroscopy, mass spectrometry, and elemental analysis. Formation constants were measured using UV-Vis spectrophotometric titration at constant ionic strength (0.10 M NaClO_4) at $25 (\pm 0.1)^\circ\text{C}$. The trend of the complex formation of Fe(III) ion with a given tridentate ligand decreases as follows:



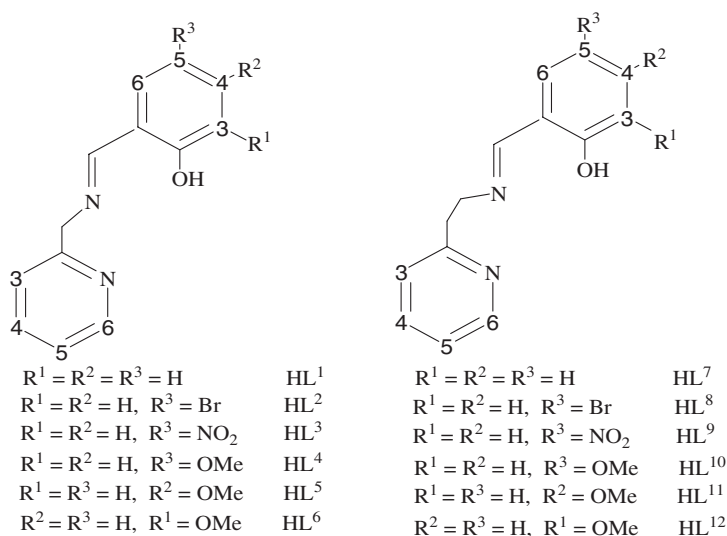
Keywords: Iron; Schiff base; Formation constant; Tridentate ligand

1. Introduction

Imino Schiff bases and their complexes have extensive literature on their use as catalysts in important industrial processes [1–6] and play a major role in coordination chemistry [7]. Thermochromism and photochromism of the ligands [8], preparation, properties, and structural aspects of some Mn [9–11], Fe [12], Co [13–15], Cu [14–17], Ni [14, 15], V [18], and Ga [12] complexes with these Schiff bases have been carried out. Comparatively little work is available on complexation and formation constants of Fe(III) compounds. Tridentate ligands, N-{pyridine-2-ylmethyl}-2-hydroxy-benzylideneamine, N-{pyridine-2-ylethyl}-2-hydroxy-benzylideneamine, and their derivatives, coordinate to Fe(III) forming bis-ligated complexes in the solid state [12].

In continuation of our previous work [19–27], we are interested in chelated complexes of tridentate ligands and Fe(III). This article describes the synthesis, characterization, and formation constants of 1 : 2 complexes of Fe^{3+} with $\text{XPh}(\text{OH})-\text{CH}=\text{N}-(\text{CH}_2)_n\text{Py}$, that $\text{X} = \text{H}, 5\text{-Br}, 5\text{-NO}_2, 5\text{-OMe}, 4\text{-OMe}, 3\text{-OMe}$, and $n = 1, 2$ (scheme 1) to

*Corresponding author. Email: asadi@susc.ac.ir



Scheme 1. Schematic representation of the ligands and labels.

understand the role played by electron-donating and -withdrawing substituents, and the coordination modes of the ligands on formation constants.

2. Experimental

2.1. Materials and physical measurements

All solvents and chemicals were purchased from Merck, Fluka or Aldrich and used without purification.

UV-Vis spectra were recorded on a Perkin-Elmer Lambda 2 instrument. FT-IR spectra were run on a Shimadzu FTIR-8300 spectrophotometer. ¹H NMR spectra were recorded on a Bruker Avance DPX-250 spectrometer in CDCl₃ or DMSO-d₆ using TMS as an internal standard at 250 MHz. Mass spectra were obtained with Shimadzu LCMS-2010EV and Perkin-Elmer R MU-6E instruments. Elemental analysis was carried out on a Thermo Finnigan-Flash-1200. The effective magnetic moment was measured using a Gouy balance.

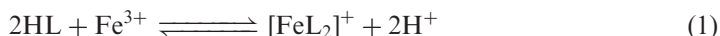
2.2. Continuous variations and molar ratio methods

For continuous variation [28] (Job's method), a series of solutions were prepared by mixing the ligand (5×10^{-5} M) and metal (5×10^{-5} M) solutions in varying proportions while keeping the total molar concentration of the mixed solutions constant.

For the molar ratio method [29], a series of solutions were prepared in which ligand concentration was kept constant (5×10^{-5} M), while that of metal ion was varied (2.5×10^{-6} – 1×10^{-4} M) for molar ratios $[M(III)]/[ligand] = 0$ – 2 . The spectra of all solutions were recorded from 200 to 800 nm.

2.3. Equilibrium measurements

Complexes were obtained from the reaction of the metal with the ligands according to equation (1).



Formation constant measurements were carried out by spectrophotometric titrations of ligands with various concentrations of the metal ion at constant ionic strength (0.10 M NaClO₄) at 25.0 (±0.1)°C. Interaction of NaClO₄ with the ligands and metal ion in methanol was negligible. In a typical measurement, 3 mL of ligand (5 × 10⁻⁵ M) in methanol was titrated with methanolic solution of Fe(NO₃)₃ · 9H₂O. Metal concentrations were varied till two-fold excess. UV-Vis spectra were recorded in the range 200–800 nm about 8 min after each addition. The absorption measurements were monitored at various wavelengths in the 500–800 nm regions where the difference in absorption between the ligands and the product was the largest after equilibrium was attained; ligand and Fe(NO₃)₃ have negligible absorptivity.

2.4. Preparation of ligands

The tridentate Schiff bases were obtained by the condensation of 2-(aminomethyl)pyridine or 2-(aminoethyl)pyridine with appropriate aldehyde: A solution of the amine (10 mmol) in MeOH (15 mL) was added to a warm solution of the appropriate aldehyde (10 mmol) in MeOH (25 mL) and the mixture was refluxed for 3 h. The solvent was removed and the product was washed with Et₂O (2 × 5 mL) (the oily product was used without further purification).

HL¹: Red oil (60%). Elemental Anal. Calcd for C₁₃H₁₂N₂O (%): C 73.57, H 5.70, N 13.20; Found (%): C 73.62, H 5.81, N 13.40. ¹H NMR (CDCl₃): δ = 13.28 (br, 1H, phOH), 8.53 (d, 4.1 Hz, 1H, py-H⁶), 8.47 (s, 1H, N=CH), 7.62 (dt, 7.7 and 1.8 Hz, 1H, py-H⁴), 7.28 (m, 3H, py-H^{3,5}, ph-H⁶), 7.14 (dt, 7.0 and 1.5 Hz, 1H, ph-H⁴), 6.94 (d, 7.0 Hz, 1H, ph-H³), 6.85 (dt, 7.0 and 1.5 Hz, 1H, ph-H⁵), 4.88 (s, 2H, CH₂) ppm. FT-IR (cm⁻¹): 3375 (O–H), 3016 (C–H), 1628 (C=N), 1589–1473 (C=C), 1215 (C–O). MS: *m/z* = 212, 195, 149, 93, 69. UV-Vis (MeOH, 25°C): λ_{max} (nm) = 212 (ε (M⁻¹ cm⁻¹) = 23,933), 261 (19,121), 318 (2690).

HL²: Yellow crystal (60%), m.p. = 79°C. Elemental Anal. Calcd for C₁₃H₁₁N₂OBr (%): C 53.63, H 3.81, N 9.62; Found (%): C 53.98, H 3.70, N 9.89. ¹H NMR (CDCl₃): δ = 13.30 (s, 1H, phOH), 8.57 (d, 4.7 Hz, 1H, py-H⁶), 8.45 (s, 1H, N=CH), 7.68 (dt, 7.6 and 1.5 Hz, 1H, py-H⁴), 7.40–7.18 (m, 4H, py-H^{3,5}, ph-H^{4,6}), 6.85 (d, 8.5 Hz, 1H, ph-H³), 4.93 (s, 2H, CH₂) ppm. FT-IR (KBr, cm⁻¹): 3433 (O–H), 3018 (C–H), 1628 (C=N), 1585–1473 (C=C), 1203 (C–O), MS: *m/z* = 291, 275, 149, 93, 65. UV-Vis (MeOH, 25°C): λ_{max} (nm) = 223 (ε (M⁻¹ cm⁻¹) = 38,543), 260 (17,831), 329 (4363).

HL³: Yellow crystal (51%), m.p. = 102°C. Elemental Anal. Calcd for C₁₃H₁₁N₃O₃ (%): C 60.70, H 4.31, N 16.33; Found (%): C 60.62, H 4.49, N 16.26. ¹H NMR (CDCl₃): δ = 14.57 (s, 1H, phOH), 8.60 (d, 6.6 Hz, 1H, py-H⁶), 8.58 (s, 1H, N=CH), 8.29 (d, 2.8 Hz, 1H, ph-H⁶), 8.20 (dd, 9.2 and 2.8 Hz, 1H, ph-H⁴), 7.72 (dt, 7.7 and 1.8 Hz, 1H, py-H⁴), 7.34 (d, 7.7 Hz, 1H, py-H³), 7.25 (m, 1H, py-H⁵), 7.99 (d, 9.2 Hz, 1H, ph-H³), 4.98 (s, 2H, CH₂) ppm. FT-IR (KBr, cm⁻¹): 3433 (O–H), 3066 (C–H), 1643 (C=N), 1539–1423

(C=C), 1261 (C–O). MS: m/z = 257, 149, 97, 73, 57. UV-Vis (MeOH, 25°C): λ_{\max} (nm) = 235 (ϵ (M⁻¹ cm⁻¹) = 18,397), 260 (24,689), 330 (11,522), 392 (8680).

HL⁴: Red oil (63%). Elemental Anal. Calcd for C₁₄H₁₄N₂O₂ (%): C 69.41, H 5.82, N 11.56; Found (%): C 69.35, H 5.90, N 11.66. ¹H NMR (CDCl₃): δ = 12.39 (s, 1H, phOH), 8.36 (d, 6.0 Hz, 1H, py-H⁶), 8.26 (s, 1H, N=CH), 7.45 (dt, 7.7 and 1.7 Hz, 1H, py-H⁴), 7.14 (d, 7.7 Hz, 1H, py-H³), 6.98 (dd, 6.2 and 2.1 Hz, 1H, ph-H⁴), 6.75 (m, 2H, py-H⁵ and ph-H⁶), 6.61 (d, 6.2 Hz, 1H, ph-H³), 4.72 (s, 2H, CH₂), 3.51 (s, 3H, OCH₃) ppm. FT-IR (cm⁻¹): 3318 (O–H), 3016 (C–H), 1635 (C=N), 1589–1488 (C=C), 1218 (C–O). MS: m/z = 242, 225, 144, 93, 57. UV-Vis (MeOH, 25°C): λ_{\max} (nm) = 227 (ϵ (M⁻¹ cm⁻¹) = 15,290), 261 (8273), 299 (2390), 346 (2250).

HL⁵: Yellow crystal (40%), m.p. (67°C). Elemental Anal. Calcd for C₁₄H₁₄N₂O₂ (%): C 69.41, H 5.82, N 11.56; Found (%): C 69.21, H 6.16, N 11.26. ¹H NMR (CDCl₃): δ = 13.79 (s, 1H, phOH), 8.57 (d, 4.4 Hz, 1H, py-H⁶), 8.40 (s, 1H, N=CH), 7.68 (dt, 7.7 and 1.6 Hz, 1H, py-H⁴), 7.34 (d, 7.7 Hz, 1H, py-H³), 7.19 (d, 8.2 Hz, 1H, ph-H⁵), 7.16 (d, 8.2 Hz, 1H, ph-H⁶), 6.44 (s, 1H, ph-H³), 6.41 (m, 1H, py-H⁵), 4.88 (s, 2H, CH₂), 3.82 (s, 3H, OCH₃) ppm. FT-IR (KBr, cm⁻¹): 3452 (O–H), 3025 (C–H), 1647 (C=N), 1519–1423 (C=C), 1223 (C–O). MS: m/z = 242, 137, 93, 65. UV-Vis (MeOH, 25°C): λ_{\max} (nm) = 217 (ϵ (M⁻¹ cm⁻¹) = 26,945), 279 (19,370), 301 (21,437), 379 (7350).

HL⁶: Yellow crystal (71%), m.p. = 101°C. Elemental Anal. Calcd for C₁₄H₁₄N₂O₂ (%): C 69.41, H 5.82, N 11.56; Found (%): C 69.73, H 5.76, N 11.82. ¹H NMR (CDCl₃): δ = 13.77 (s, 1H, phOH), 8.55 (d, 4.9 Hz, 1H, py-H⁶), 8.53 (s, 1H, N=CH), 7.66 (dt, 7.7 and 1.7 Hz, 1H, py-H⁴), 7.37 (d, 7.7 Hz, 1H, py-H³), 7.26 (d, not resolved, 1H, ph-H⁶), 7.18 (dd, 6.3 Hz, not resolved, 1H, ph-H⁴), 6.93 (dd, 6.3 and 1.9 Hz, 1H, ph-H⁵), 6.82 (dd, 7.7 Hz, not resolved, 1H, py-H⁵), 4.95 (s, 2H, CH₂), 3.87 (s, 3H, OCH₃) ppm. FT-IR (KBr, cm⁻¹): 3414 (O–H), 3009 (C–H), 1635 (C=N), 1589–1466 (C=C), 1254 (C–O). MS: m/z = 242, 167, 149, 93, 57. UV-Vis (MeOH, 25°C): λ_{\max} (nm) = 221 (ϵ (M⁻¹ cm⁻¹) = 21,614), 262 (14,758), 325 (2172).

HL⁷: Red oil (55%). Elemental Anal. Calcd for C₁₄H₁₄N₂O (%): C 74.31, H 6.24, N 12.38; Found (%): C 74.23, H 6.36, N 12.19. ¹H NMR (CDCl₃): δ = 13.11 (br, 1H, phOH), 8.56 (d, 4.8 Hz, 1H, py-H⁶), 8.28 (s, 1H, N=CH), 7.59 (dt, 7.6 and 1.2 Hz, 1H, py-H⁴), 7.30–7.10 (m, 4H, py-H^{3,5}, ph-H^{4,6}), 6.90 (d, 8.3 Hz, 1H, ph-H³), 6.84 (t, 7.4 Hz, 1H, ph-H⁵), 4.02 (t, 6.9 Hz, 2H, CH₂N), 3.17 (t, 6.9 Hz, 2H, CH₂) ppm. FT-IR (cm⁻¹): 3394 (O–H), 3009 (C–H), 1628 (C=N), 1589–1496 (C=C), 1211 (C–O). MS: m/z = 226, 106, 51. UV-Vis (MeOH, 25°C): λ_{\max} (nm) = 214 (ϵ (M⁻¹ cm⁻¹) = 27,812), 260 (24,447), 319 (4574).

HL⁸: Yellow crystal (52%), m.p. (72°C). Elemental Anal. Calcd for C₁₄H₁₃N₂OBr (%): C 55.10, H 4.29, N 9.18; Found (%): C 55.34, H 4.12, N 9.23. ¹H NMR (CDCl₃): δ = 13.37 (s, 1H, phOH), 8.56 (d, 2.9 Hz, 1H, py-H⁶), 8.18 (s, 1H, N=CH), 7.59–6.78 (m, 6H, py-H^{3,4,5}, ph-H^{3,4,6}), 4.03 (t, 6.8 Hz, 2H, CH₂N), 3.15 (t, 6.8 Hz, 2H, CH₂) ppm. FT-IR (KBr, cm⁻¹): 3425 (O–H), 3023 (C–H), 1635 (C=N), 1589–1473 (C=C), 1280 (C–O). MS: m/z = 305, 289, 225, 185, 149, 106, 51. UV-Vis (MeOH, 25°C): λ_{\max} (nm) = 222 (ϵ (M⁻¹ cm⁻¹) = 43,617), 254 (16,418), 324 (4028).

HL⁹: Yellow crystal (86%), m.p. (158°C). Elemental Anal. Calcd for C₁₄H₁₃N₃O₃ (%): C 61.99, H 4.83, N 15.49; Found (%): C 62.23, H 4.72, N 15.59. ¹H NMR (DMSO-*d*₆): δ = 14.17 (s, 1H, phOH), 8.70 (s, 1H, N=CH), 8.52 (d, 4.8 Hz, 1H, py-H⁶), 8.35

(d, 3.1 Hz, 1H, ph-H⁶), 8.00 (dd, 9.6 and 3.1 Hz, 1H, ph-H⁴), 7.72 (dt, 7.7 and 1.8 Hz, 1H, py-H⁴), 7.30 (d, 7.7 Hz, 1H, py-H³), 7.24 (m, 1H, py-H⁵), 6.56 (d, 9.6 Hz, 1H, ph-H³), 4.06 (t, 6.7 Hz, 2H, CH₂N), 3.19 (t, 6.7 Hz, 2H, CH₂) ppm. FT-IR (KBr, cm⁻¹): 3440 (O-H), 3047 (C-H), 1666 (C=N), 1535–1435 (C=C), 1218 (C-O). MS: *m/z* = 271, 255, 106, 51. UV-Vis (MeOH, 25°C): λ_{max} (nm) = 235 (ε (M⁻¹ cm⁻¹) = 17,398), 260 (29,925), 345 (14,023), 393 (12,396).

HL¹⁰: Red oil (59%). Elemental Anal. Calcd for C₁₅H₁₆N₂O₂ (%): C 70.29, H 6.29, N 10.93; Found (%): C 70.38, H 6.18, N 11.07. ¹H NMR (CDCl₃): δ = 12.36 (s, 1H, phOH), 8.46 (d, 4.4 Hz, 1H, py-H⁶), 8.14 (s, 1H, N=CH), 7.48 (m, 1H, py-H⁴), 7.04 (m, 2H, py-H^{3,5}), 6.81 (m, 2H, ph-H^{4,6}), 6.61 (d, 2.5 Hz, 1H, ph-H³), 3.91 (t, 6.5 Hz, 2H, CH₂N), 3.63 (s, 3H, OCH₃), 3.06 (t, 6.5 Hz, 2H, CH₂) ppm. FT-IR (cm⁻¹): 3394 (O-H), 3016 (C-H), 1635 (C=N), 1589–1497 (C=C), 1265 (C-O). MS: *m/z* = 265, 151, 106, 51. UV-Vis (MeOH, 25°C): λ_{max} (nm) = 229 (ε (M⁻¹ cm⁻¹) = 58,496), 260 (28,624), 343 (10,367).

HL¹¹: Yellow crystal (58%), m.p. (52°C). Elemental Anal. Calcd for C₁₅H₁₆N₂O₂ (%): C 70.29, H 6.29, N 10.93; Found (%): C 70.13, H 6.35, N 11.12. ¹H NMR (CDCl₃): δ = 13.69 (s, 1H, phOH), 8.44 (d, 4.4 Hz, 1H, py-H⁶), 7.95 (s, 1H, N=CH), 7.44 (dt, 7.6 and 1.5 Hz, 1H, py-H⁴), 7.02 (d, 7.6 Hz, 1H, py-H³), 6.98 (m, 1H, py-H⁵), 6.89 (d, 8.5 Hz, 1H, ph-H⁶), 6.27 (d, 2.2 Hz, 1H, ph-H³), 6.20 (dd, 8.5 and 2.2 Hz, 1H, ph-H⁵), 3.81 (t, 6.9 Hz, 2H, CH₂N), 3.62 (s, 3H, OCH₃), 3.01 (t, 6.9 Hz, 2H, CH₂) ppm. FT-IR (cm⁻¹): 3433 (O-H), 3018 (C-H), 1623 (C=N), 1508–1465 (C=C), 1223 (C-O). MS: *m/z* = 256, 151, 106, 51. UV-Vis (MeOH, 25°C): λ_{max} (nm) = 218 (ε (M⁻¹ cm⁻¹) = 25,064), 251 (15,790), 297 (21,620), 378 (9620).

HL¹²: Red oil (75%). Elemental Anal. Calcd for C₁₅H₁₆N₂O₂ (%): C 70.29, H 6.29, N 10.93; Found (%): C 70.22, H 6.41, N 10.78. ¹H NMR (CDCl₃): δ = 13.70 (s, 1H, phOH), 8.46 (d, 4.6 Hz, 1H, py-H⁶), 8.17 (s, 1H, N=CH), 7.49 (dt, 7.6 and 1.7 Hz, 1H, py-H⁴), 7.07 (m, 2H, py-H^{3,5}), 6.80 (dd, 7.2 and 2.3 Hz, 1H, ph-H⁴), 6.71 (m, 2H, ph-H^{5,6}), 3.94 (t, 6.7 Hz, 2H, CH₂N), 3.79 (s, 3H, OCH₃), 3.08 (t, 6.7 Hz, 2H, CH₂) ppm. FT-IR (cm⁻¹): 3414 (O-H), 3009 (C-H), 1635 (C=N), 1589–1466 (C=C), 1254 (C-O). MS: *m/z* = 256, 137, 106, 57. UV-Vis (MeOH, 25°C): λ_{max} (nm) = 220 (ε (M⁻¹ cm⁻¹) = 15,333), 261 (9758), 293 (4114), 334 (1523).

2.5. Preparation of [Fe^{III}(L^X)₂]ClO₄ complexes

A general synthetic route was used for X = 1–12 in which a solution of Fe(NO₃)₃·9H₂O (1.0 mmol) in MeOH (10 mL) was added to a 30 mL MeOH solution containing the appropriate ligand (2.0 mmol) and Et₃N (2.0 mmol). The resulting dark solution was refluxed for 2 h, the mixture was filtered while warm and excess NaClO₄ was added to exchange nitrate by perchlorate. After 24 h, dark microcrystalline precipitates were filtered, washed with H₂O, cold MeOH, and Et₂O.

Caution: Although no difficulties were experienced, all complexes were isolated as their perchlorate salts, and therefore, they should be handled as potentially explosive compounds.

[Fe(L¹)₂]ClO₄·MeOH. Yield: 45%. m.p. >250°C. Elemental Anal. Calcd for C₂₇H₂₆N₄O₇ClFe (%): C 53.18, H 4.30, N 9.19; Found (%): C 52.95, H 4.08,

N 8.91. FT-IR (KBr, cm^{-1}): 1616 (C=N), 1539–1442 (C=C), 1296 (C–O), 1095 (O–ClO₃). MS (ESI(+)) in MeOH:H₂O): m/z 478 for [Fe(L¹)₂]⁺. UV-Vis (MeOH, 25°C): λ_{max} (nm) = 233 (ϵ ($\text{M}^{-1}\text{cm}^{-1}$) = 43,062), 261 (32,771), 323 (12,640), 510 (3443).

[Fe(L²)₂]ClO₄. Yield: 44%. m.p. = 246°C. Elemental Anal. Calcd for C₂₆H₂₀N₄O₆Br₂ClFe (%): C 42.45, H 2.74, N 7.62; Found (%): C 42.51, H 2.77, N 7.68. FT-IR (KBr, cm^{-1}): 1620 (C=N), 1524–1454 (C=C), 1280 (C–O), 1095 (O–ClO₃). MS (ESI(+)) in MeOH:H₂O): m/z 636 for [Fe(L²)₂]⁺. UV-Vis (MeOH, 25°C): λ_{max} (nm) = 218 (ϵ ($\text{M}^{-1}\text{cm}^{-1}$) = 49,452), 234 (47,463), 349 (9258), 525 (3138).

[Fe(L³)₂]ClO₄. Yield: 32%. m.p. > 250°C. Elemental Anal. Calcd for C₂₆H₂₀N₆O₁₀ClFe (%): C 46.76, H 3.02, N 12.59; Found (%): C 46.98, H 3.35, N 12.33. FT-IR (KBr, cm^{-1}): 1624 (C=N), 1547–1469 (C=C), 1308 (C–O), 1095 (O–ClO₃). MS (ESI(+)) in MeOH:H₂O): m/z 568 for [Fe(L³)₂]⁺. UV-Vis (MeOH, 25°C): λ_{max} (nm) = 220 (ϵ ($\text{M}^{-1}\text{cm}^{-1}$) = 58,967), 241 (51,385), 340 (39,888), 520 (4010).

[Fe(L⁴)₂]ClO₄·2H₂O. Yield: 38%. m.p. = 180°C. Elemental Anal. Calcd for C₂₈H₃₀N₄O₁₀ClFe (%): C 50.21, H 4.17, N 8.39; Found (%): C 50.36, H 4.25, N 8.61. FT-IR (KBr, cm^{-1}): 1608 (C=N), 1539–1466 (C=C), 1288 (C–O), 1095 (O–ClO₃). MS (ESI(+)) in MeOH:H₂O): m/z 538 for [Fe(L⁴)₂]⁺. UV-Vis (MeOH, 25°C): λ_{max} (nm) = 214 (ϵ ($\text{M}^{-1}\text{cm}^{-1}$) = 94,580), 242 (89,534), 382 (16,610), 575 (7067).

[Fe(L⁵)₂]ClO₄·Et₂O. Yield: 35%. m.p. = 141°C. Elemental Anal. Calcd for C₃₂H₃₆N₄O₉ClFe (%): C 53.70, H 5.10, N 7.83; Found (%): C 53.67, H 4.99, N 7.56. FT-IR (KBr, cm^{-1}): 1601 (C=N), 1527–1404 (C=C), 1223 (C–O), 1095 (O–ClO₃). MS (ESI(+)) in MeOH:H₂O): m/z 538 for [Fe(L⁵)₂]⁺. UV-Vis (MeOH, 25°C): λ_{max} (nm) = 245 (ϵ ($\text{M}^{-1}\text{cm}^{-1}$) = 41,415), 283 (43,543), 343 (14,300), 525 (3935).

[Fe(L⁶)₂]ClO₄. Yield: 46%. m.p. > 250°C. Elemental Anal. Calcd for C₂₈H₂₆N₄O₈ClFe (%): C 53.00, H 4.32, N 8.58; Found (%): C 53.00, H 4.65, N 8.78. FT-IR (KBr, cm^{-1}): 1608 (C=N), 1551–1435 (C=C), 1223 (C–O), 1095 (O–ClO₃). MS (ESI(+)) in MeOH:H₂O): m/z 538 for [Fe(L⁶)₂]⁺. UV-Vis (MeOH, 25°C): λ_{max} (nm) = 226 (ϵ ($\text{M}^{-1}\text{cm}^{-1}$) = 58,431), 273 (39,254), 350 (11,390), 550 (3910).

[Fe(L⁷)₂]ClO₄·H₂O. Yield: 48%. m.p. = 227°C. Elemental Anal. Calcd for C₂₈H₂₈N₄O₇ClFe (%): C 53.91, H 4.52, N 8.98; Found (%): C 53.67, H 4.31, N 8.83. FT-IR (KBr, cm^{-1}): 1608 (C=N), 1542–1446 (C=C), 1299 (C–O), 1095 (O–ClO₃). MS (ESI(+)) in MeOH:H₂O): m/z 506 for [Fe(L⁷)₂]⁺. UV-Vis (MeOH, 25°C): λ_{max} (nm) = 210 (ϵ ($\text{M}^{-1}\text{cm}^{-1}$) = 53,524⁻¹), 234 (45,546), 260 (37,180), 324 (11,341), 551 (3549).

[Fe(L⁸)₂]ClO₄·H₂O. Yield: 64%. m.p. = 236°C. Elemental Anal. Calcd for C₂₈H₂₆N₄O₆Br₂ClFe (%): C 43.03, H 3.35, N 7.17; Found (%): C 43.27, H 3.24, N 7.02. FT-IR (KBr, cm^{-1}): 1608 (C=N), 1531–1454 (C=C), 1384 (C–O), 1095 (O–ClO₃). MS (ESI(+)) in MeOH:H₂O): m/z 664 for [Fe(L⁸)₂]⁺. UV-Vis (MeOH, 25°C): λ_{max} (nm) = 221 (ϵ ($\text{M}^{-1}\text{cm}^{-1}$) = 77,273), 330 (12,511), 543 (3160).

[Fe(L⁹)₂]ClO₄·MeOH. Yield: 58%. m.p. = 244°C. Elemental Anal. Calcd for C₂₉H₂₈N₆O₁₁ClFe (%): C 47.85, H 3.88, N 11.55; Found (%): C 47.56, H 3.82, N 11.83. FT-IR (KBr, cm^{-1}): 1605(C=N), 1558–1466 (C=C), 1315 (C–O), 1095 (O–ClO₃). MS (ESI(+)) in MeOH:H₂O): m/z 596 for [Fe(L⁹)₂]⁺. UV-Vis (MeOH, 25°C): λ_{max} (nm) = 227 (ϵ ($\text{M}^{-1}\text{cm}^{-1}$) = 50,915), 244 (54,593), 343 (36,552), 480 (3728).

[Fe(L¹⁰)₂]ClO₄. Yield: 69%. m.p. = 224°C. Elemental Anal. Calcd for C₃₀H₃₀N₄O₈ClFe (%): C 54.11, H 4.54, N 8.41; Found: C 54.21, H 4.72, N 8.75. FT-IR (KBr, cm⁻¹): 1605 (C=N), 1546–1446 (C=C), 1249 (C–O), 1095 (O–ClO₃). MS (ESI(+) in MeOH:H₂O): *m/z* 566 for [Fe(L¹⁰)₂]⁺. UV-Vis (MeOH, 25°C): λ_{max} (nm) = 210 (ε (M⁻¹ cm⁻¹) = 53,365), 241 (60,235), 348 (12,822), 631 (4942).

[Fe(L¹¹)₂]ClO₄. Yield: 38%. m.p. = 165°C. Elemental Anal. Calcd for C₃₀H₃₀N₄O₈ClFe (%): C 54.11, H 4.54, N 8.41; Found (%): C 53.85, H 4.65, N 8.37. FT-IR (KBr, cm⁻¹): 1597 (C=N), 1531–1443 (C=C), 1230 (C–O), 1095 (O–ClO₃). MS (ESI(+) in MeOH:H₂O): *m/z* 566 for [Fe(L¹¹)₂]⁺. UV-Vis (MeOH, 25°C): λ_{max} (nm) = 246 (ε (M⁻¹ cm⁻¹) = 63,858), 281 (64,638), 380 (11,159), 560 (5289).

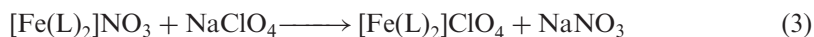
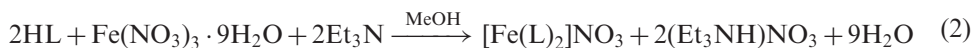
[Fe(L¹²)₂]ClO₄·H₂O. Yield: 81%. m.p. = 233°C. Elemental Anal. Calcd for C₃₀H₃₂N₄O₉ClFe (%): C 52.69, H 4.72, N 8.20; Found (%): C 52.73, H 4.59, N 8.59. FT-IR (KBr, cm⁻¹): 1605 (C=N), 1547–1446 (C=C), 1249 (C–O), 1095 (O–ClO₃). MS (ESI(+) in MeOH:H₂O): *m/z* 566 for [Fe(L¹²)₂]⁺. UV-Vis (MeOH, 25°C): λ_{max} (nm) = 230 (ε (M⁻¹ cm⁻¹) = 47,320), 267 (49,764), 350 (7194), 600 (2895).

3. Results and discussion

3.1. Synthesis and characterization

Reaction of 2-(2-aminomethyl)pyridine or 2-(2-aminoethyl)pyridine with one molar equivalent of substituted salicylaldehyde in refluxing MeOH afforded a yellow solution. Evaporation of this solution to dryness yielded ligands in good yields and are characterized by ¹H NMR, FTIR, UV-Vis spectroscopy, mass spectrometry, and elemental analysis.

Complexes were synthesized by treating the respective ligand with iron(III) nitrate nonahydrate in dry methanol, followed by counterion metathesis with sodium perchlorate (equations (2) and (3)).



The elemental analyses are in agreement with the calculated values for 1:2 metal to ligand ratio.

Based on the crystal structures of related complexes [12, 30], one may conclude that these reactions yielded pseudo-octahedral mononuclear species in which iron is surrounded by two tridentate ligands. Imbert *et al.* [12] showed that iron(III) is positioned in a distorted octahedral N₂N'₂O₂ environment with high spin 3d⁵ configuration.

3.2. Infrared spectroscopy, mass spectrometry

Weak bands at 2800–3100 cm⁻¹ are related to (C–H) vibrations. The imine ligands show a C=N peak around 1630 cm⁻¹ that shifts to lower frequencies upon coordination,

indicating nitrogen of azomethine coordinates to iron. The C=C bond was at 1450–1600 cm^{-1} and perchlorate counterions were found between 1116 and 1088 cm^{-1} .

The ESI mass spectrometry in positive mode in 1 : 1 MeOH/H₂O gave single, well-defined peaks corresponding to $m/z = [\text{M}^{\text{III}}(\text{L})_2]^+$ for all complexes. A typical mass spectrum of $\text{Fe}(\text{L}^{11})_2^+$ (Mw = 566) is provided in “Supplementary material”.

3.3. Electronic absorption spectra, magnetic moment, and stoichiometry of the complexes formed in solution

The electronic spectra of the ligands and complexes were measured in methanol to compare differences between the ligands and complexes. Figure 1 shows spectra for comparisons. All ligands show interligand $\pi \rightarrow \pi^*$ bands around 220 and 260 nm attributed to pyridine and phenolate moieties. Another band attributed to the $n \rightarrow \pi^*$ groups is observed around 330 nm.

The electronic spectra of complexes show two absorptions around 340 and 600 nm. Transitions $p\pi_{\text{phenolate}} \rightarrow d\pi^*_{\text{iron(III)}}$ are associated to the band at 600 nm, whereas the higher-energy absorption at 340 nm is attributed to a $p\pi_{\text{phenolate}} \rightarrow d\sigma^*_{\text{iron(III)}}$ LMCT process [12].

Magnetic moment values, μ_{eff} , were measured for 12 solid complexes by Gouy balance (Supplementary material). The μ_{eff} values (5.9 B.M.) indicate that the Fe^{3+} ion is high spin [12], ruling out d–d transitions in the visible spectra.

To determine the stoichiometry of the different complexes formed in solution from the interaction of Fe(III) with HL¹–HL¹², two different spectrophotometric methods, continuous variation (CV) [28], and molar ratio (MR) of Yoe and Jones [29] have been applied.

Changes in the absorbance spectra of HL¹¹ at different molar ratio of the Fe(III) added in methanol (molar ratio experiment) are shown in figure 2. The presence of two isosbestic points suggests two equilibria with 1 : 1 and 1 : 2 species.

The resulting molar ratio and continuous variation plots for this system are shown in figure 3. The relationship obtained for the MR method are characterized by one break at molar ratio $[\text{M}]/[\text{L}]$ equals to 0.5, indicating that the stoichiometry of the complexes

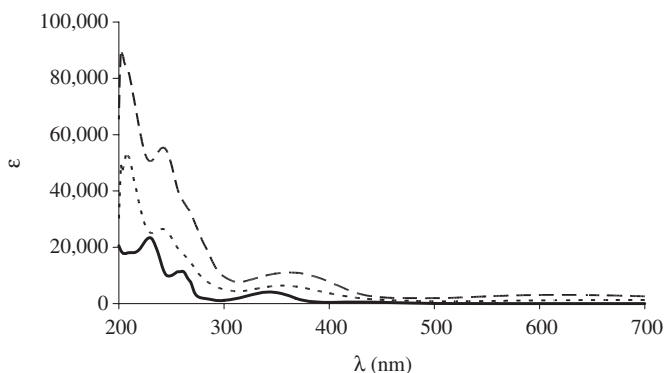


Figure 1. UV-Vis spectra of HL¹⁰(—) (5.0×10^{-5} M), $\text{Fe}(\text{L}^{10})_2\text{ClO}_4$ separately synthesized (---) (2.0×10^{-5} M), and the product at the end of titration (...) (M : L = 1 : 2).

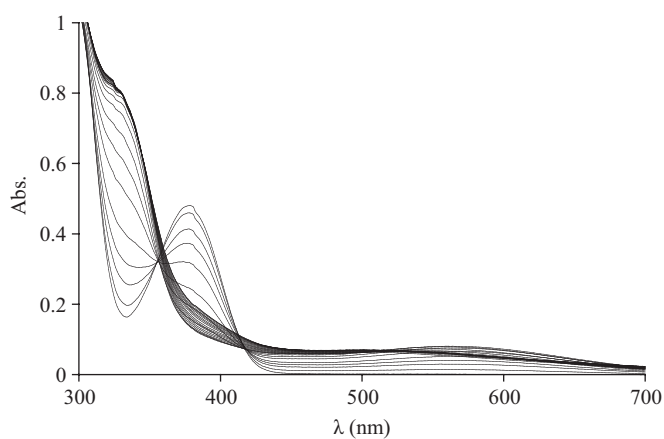


Figure 2. Spectrophotometric titration of HL¹¹ (5.0×10^{-5} M) with various amounts of $\text{Fe}(\text{NO}_3)_3 \cdot 9\text{H}_2\text{O}$ (2.5×10^{-6} – 1×10^{-4} M) in methanol ($I=0.10$ M at 25°C).

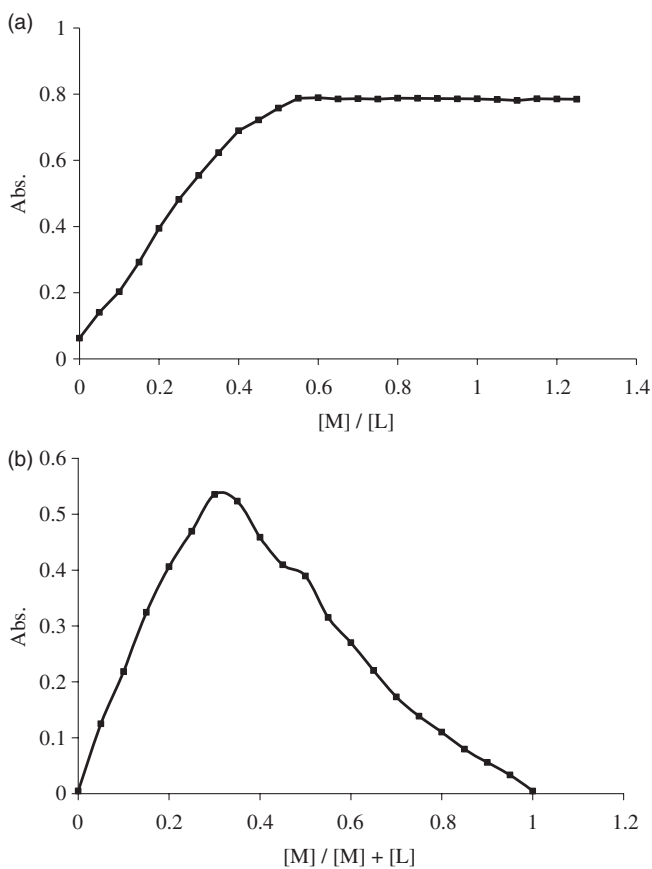


Figure 3. Molar ratio ($L = 5.0 \times 10^{-5}$ M and $M = 2.5 \times 10^{-6}$ – 1×10^{-4} M) (a) and continuous variation ($L = 5.0 \times 10^{-5}$ M and $M = 5.0 \times 10^{-5}$ M that vary proportions); (b) plots of HL¹¹ with $\text{Fe}(\text{NO}_3)_3 \cdot 9\text{H}_2\text{O}$ in methanol at 25°C at $\lambda = 400$ nm.

is 1 : 2 (M : L). Results of the CV method support the results of the MR method. Curves plotted for CV method are characterized by one clear maximum at metal mole fraction equal to ~ 0.33 , for most cases, or by a shoulder accompanied by a maximum located also at the same metal mole fraction value, i.e. 0.33 and/or 0.5. This behavior clearly indicates that the stoichiometry of the different complexes formed in the solution from the reaction of the Fe^{3+} ions with ligands ($\text{HL}^1\text{--HL}^{12}$) is 1 : 2 and/or 1 : 1 (M : L).

3.4. Evaluation of the formation constants and Gibbs free energy of the different metal chelates

The data obtained from the molar ratio spectrophotometric method, used to establish the stoichiometry of the metal complexes, were also utilized for the determination of the formation constants.

The formation constants, K_1 and K_2 , were calculated using the SQUAD computer program [31, 32], designed to calculate the best value for the formation constants of the proposed model (equation (1)) by employing a non-linear, least-squares approach. Also, the free energy changes ΔG^0 of the formed complexes were calculated from $\Delta G^0 = -RT \ln K$ at 25°C.

The K_1 and K_2 values and Gibbs free energies obtained for the metal complexes under investigation are given in table 1. These data show that there was more difference between K_1 and K_2 values. By considering concentration distribution curves for Fe(III) species in solution, it was clear that the formation of mono complexes would be negligible due to the mono complexes converting to bis complexes immediately. The bis complexes with two tridentate chelating ligands have octahedral geometry preferred over the mono complex with one ligand and three monodentate solvent molecules.

The $\log K$ values for Fe(II) and Fe(III) complexes, carried out by other workers, show vast differences due to the kind and number of ligands [33–37]. According to the electronic and steric effects, K_1 must be larger than K_2 [33, 34], but sometimes K_2 can be larger than K_1 because of the chelating effect, structural reason, and so on [35, 36].

Our formation constants and Gibbs free energies follow the sequence:

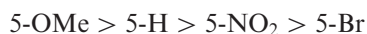


Table 1. Formation constants ($\log K_1$ and $\log K_2$) and Gibbs free energy (ΔG_1^0 and ΔG_2^0) for the complexes of tridentate ligands with Fe(III) in methanol ($I=0.10$ M at 25°C).

	$\log K_1$	$\log K_2$	ΔG_1^0 (kJ mol ⁻¹)	ΔG_2^0 (kJ mol ⁻¹)
HL ¹	3.81 (± 0.04)	9.62 (± 0.07)	-21.7 (± 0.1)	-54.9 (± 0.2)
HL ²	3.15 (± 0.09)	9.15 (± 0.05)	-18.0 (± 0.2)	-52.2 (± 0.1)
HL ³	3.47 (± 0.07)	9.47 (± 0.06)	-19.8 (± 0.2)	-54.0 (± 0.1)
HL ⁴	4.02 (± 0.09)	9.72 (± 0.08)	-22.9 (± 0.2)	-55.4 (± 0.2)
HL ⁵	3.83 (± 0.05)	9.43 (± 0.06)	-21.8 (± 0.1)	-53.8 (± 0.1)
HL ⁶	3.61 (± 0.02)	9.31 (± 0.08)	-20.59 (± 0.05)	-53.1 (± 0.2)
HL ⁷	3.91 (± 0.08)	9.77 (± 0.09)	-22.3 (± 0.2)	-55.7 (± 0.2)
HL ⁸	3.33 (± 0.05)	9.45 (± 0.06)	-19.0 (± 0.1)	-53.9 (± 0.1)
HL ⁹	3.54 (± 0.09)	9.60 (± 0.07)	-20.2 (± 0.2)	-54.7 (± 0.2)
HL ¹⁰	4.11 (± 0.07)	10.09 (± 0.09)	-23.4 (± 0.2)	-57.6 (± 0.2)
HL ¹¹	3.99 (± 0.08)	9.8 (± 0.1)	-22.7 (± 0.2)	-56.0 (± 0.2)
HL ¹²	3.78 (± 0.07)	9.68 (± 0.08)	-21.6 (± 0.2)	-55.2 (± 0.2)

In the *para* substituted Schiff-base ligands, the stability constants and Gibbs free energies vary as expected from electronic effects of the substituents decreasing according to the sequence $\text{OCH}_3 > \text{H} > \text{Br} > \text{NO}_2$, i.e., in order of an increase in both electron-withdrawing and π -acceptor qualities of the substituents and the decrease in donor ability of the ligand groups (mainly the phenoxy groups). This is somewhat in agreement with the cited sequence, except for 5- NO_2 that was attributed to the hydrogen bonding between NO_2 group and $\text{N}=\text{CH}$.

The log K values (table 1) show that electron-donating groups (such as OMe) in the *para* position to OH of the Schiff-base complex bind more strongly with Fe(III). Conversely, electron-withdrawing groups such as NO_2 bind more weakly. This behavior confirms the results obtained in the recent work [38, 39] related to adducts between different substituted Schiff-base complexes of Ni(II) and Cu(II) with organotin(IV) dichloride. Also, our previous work on thermodynamics of different types of Co(III) Schiff-base complexes as acceptor with donors such as phosphites [20, 24, 40] and amines [21, 26] agrees with our present work on Fe(III) Schiff-base complexes.

To study the effect of the position of substituents on the formation of the complexes, 3-OMe, 4-OMe, and 5-OMe were selected. The results show the following trend in the complex formation between iron and the tridentate ligand



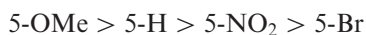
related to the steric effects of substituted ligands.

4. Conclusion

Our results confirm the results of the recently published work. The stability of the bidentate and tridentate Schiff-base complexes depends on the metal, the type of Schiff base, and the substituent groups. Some complexes play efficient catalytic roles in organic reactions, specially those of coordinated Fe(III) complexes, and some with heterocyclic compounds are essential to many biochemical processes.

Heterocyclic tridentate ligands (NNO) with different substituents coordinate with Fe(III) cations mainly by 2:1 mole ratio. Variations of stability constant of the complexes formed verify the electronic and the position of the substituents.

The free energy of formation of the 12 iron Schiff-base complexes show the electronic effect of the substituent groups, i.e.,



The position of the methoxy substituent can also affect the K and the ΔG^0 values and the following trend was observed:



Acknowledgement

We are grateful to Shiraz University Research Council for their financial support.

References

- [1] A.A. Aly, K.M. Elshaieb. *Tetrahedron*, **60**, 3797 (2004).
- [2] M.J. Bu, Z.M.A. Judeh, C.B. Ching, S. Kawi. *Catal. Lett.*, **85**, 183 (2003).
- [3] K.C. Gupta, H.K. Abdulkadir, S. Chand. *J. Macromol. Sci. Part A Pure Appl. Chem.*, **39**, 1451 (2002).
- [4] B. Gigante, A. Corma, H. Garcia, M.J. Sabater. *Catal. Lett.*, **68**, 113 (2000).
- [5] M. Nath, H. Singh, G. Eng, X. Song. *J. Organomet. Chem.*, **693**, 2541 (2008).
- [6] S. Rayati, N. Torabi, A. Chaemi, S. Mohebbi, A. Wojtczak, A. Kozakiewicz. *Inorg. Chim. Acta*, **361**, 1239 (2008).
- [7] D.A. Atwood. *Coord. Chem. Rev.*, **165**, 267 (1997).
- [8] E. Lambi, D. Gegiou, E. Hadjoudis. *J. Photochem. Photobiol. A*, **86**, 241 (1995).
- [9] F.C. Frederick, W.M. Coleman, L.T. Taylor. *Inorg. Chem.*, **22**, 792 (1983).
- [10] B. Mabad, P. Cassoux, J.P. Tuchagues, D.N. Hendrickson. *Inorg. Chem.*, **25**, 1420 (1986).
- [11] S. Theil, R. Yerande, R. Chikate, F. Dahan, A. Bousseksou, S. Padhye, J.P. Tuchagues. *Inorg. Chem.*, **36**, 6279 (1997).
- [12] C. Imbert, H.P. Hratchian, M. Lanznaster, M.J. Heeg, L.M. Hryhorczuk, B.R. McGarvey, H.B. Schlegel, C.N. Verani. *Inorg. Chem.*, **44**, 7414 (2005).
- [13] R. Shakya, S.S. Hindo, L. Wu, M.M. Allard, M.J. Heeg, H.P. Hratchian, B.R. McGarvey, S.R.P. da Rocha, C.N. Verani. *Inorg. Chem.*, **46**, 9808 (2007).
- [14] S.K. Padhi, V. Manivannan. *Polyhedron*, **26**, 1619 (2007).
- [15] S.K. Padhi, V. Manivannan. *Polyhedron*, **26**, 3092 (2007).
- [16] W.E. Hatfield, F. Buncer. *Inorg. Chem.*, **8**, 1194 (1969).
- [17] P. Li, N.K. Solanki, H. Ehrenberg, N. Feeder, J.E. Davies, J.M. Rawson, M.A. Halcrow. *J. Chem. Soc., Dalton Trans.*, 1559 (2000).
- [18] B. Baruah, S.P. Rath, A. Chakravorty. *Eur. J. Inorg. Chem.*, **9**, 1873 (2004).
- [19] M. Asadi, Kh. Mohammadi, A.H. Kianfar. *J. Iran. Chem. Soc.*, **3**, 247 (2006).
- [20] M. Asadi, A.H. Sarvestani, Z. Asadi, M. Setoodehkhah. *Metal Org. Chem.*, **35**, 639 (2005).
- [21] M. Asadi, A.H. Kianfar, S. Torabi, Kh. Mohammadi. *J. Chem. Thermodyn.*, **40**, 523 (2008).
- [22] M. Asadi, A.H. Kianfar, M. Abbasi. *J. Chem. Res. (S)*, 56 (2007).
- [23] M. Asadi, Z. Asadi. *J. Coord. Chem.*, **61**, 640 (2008).
- [24] M. Asadi, A.H. Sarvestani. *Can. J. Chem.*, **79**, 1360 (2001).
- [25] M. Asadi, A.H. Sarvestani. *J. Chem. Res. (S)*, 520 (2002).
- [26] M. Asadi, A.H. Sarvestani, M.B. Ahmadi, Kh. Mohammadi, Z. Asadi. *J. Chem. Thermodyn.*, **36**, 141 (2004).
- [27] M. Asadi, Kh. Aein Jamshid, A.H. Kianfar. *J. Coord. Chem.*, **61**, 1115 (2007).
- [28] P. Job. *Ann. Chem. Phys.*, **2**, 113 (1928).
- [29] J.H. Yoe, A.L. Jones. *Ind. Eng. Chem. Analyst*, **16**, 45 (1944).
- [30] C.R. Kowol, R. Berger, R. Eichinger, A. Roller, M.A. Jakupec, P.P. Schmidt, V.B. Arion, B.K. Keppler. *J. Med. Chem.*, **50**, 1254 (2007).
- [31] D.L. Leggett. *Computational Methods for the Determination of Formation Constant*, Plenum Press, New York (1985).
- [32] D.K. Dey, M.K. Saha, M. Gielen, M. Kemmer, M. Biesemans, R. Willem, V. Gramlich, S. Mitra. *J. Organomet. Chem.*, **590**, 88 (1999).
- [33] M. Enamullah, W. Linert. *Thermochim. Acta*, **388**, 401 (2002).
- [34] M.S. Masoud, H.H. Hammud, H. Beidas. *Thermochim. Acta*, **381**, 119 (2000).
- [35] M.A. Santos, M. Gil, S. Marques, L. Gano, G. Cantinho, S. Chaves. *J. Inorg. Biochem.*, **92**, 43 (2002).
- [36] L.C. Konigsberger, E. Konigsberger, P.M. May, G.T. Hefter. *J. Inorg. Biochem.*, **78**, 175 (2000).
- [37] M. Borsari, E. Ferrari, R. Grandi, M. Saladini. *Inorg. Chim. Acta*, **328**, 61 (2002).
- [38] K. Aein Jamshid, M. Asadi, A.H. Kianfar. *J. Coord. Chem.*, **62**, 1187 (2009).
- [39] A.H. Kianfar, M. Mosalla Nejad. *J. Coord. Chem.*, **62**, 3232 (2009).
- [40] M. Asadi, Z. Asadi. *Transition Met. Chem.*, **32**, 387 (2007).